HHS Public Access

Author manuscript

*Placenta*. Author manuscript; available in PMC 2024 September 25.

Published in final edited form as:

*Placenta*. 2022 August ; 126: 17–25. doi:10.1016/j.placenta.2022.05.005.

# Targeted disruption of Gdi2 causes early embryonic lethality

**Yin Wu**,

**Darong Yang**,

**Guo-Yun Chen***

Children's Foundation Research Institute at Le Bonheur Children's Hospital, Department of Pediatrics, University of Tennessee Health Science Center, Memphis, TN, 38103, USA

## Abstract

**Introduction:** GDI2 regulates the GDP/GTP exchange reaction of Rab proteins by inhibiting the dissociation of GDP and the subsequent binding of GTP, dysregulation of GDI2 has been reported in many different cancers. Recently, we found that GDI2 bound to the ITIM domain of Siglec-G under normal homeostasis, whereas Rab1a was recruited to the ITIM domain during bacterial infection. Therefore, GDI2 and Rab1a may regulate the immune response through interaction with the ITIM domain during bacterial infection. However, the regulation of the inflammatory response by GDI2 in vivo and its regulatory mechanism remain unknown.

**Methods:** We generated a *Gdi2* null mutant mouse with a trapped *Gdi2* gene and examined the expression by X-gal and immunohistochemistry staining. TUNEL staining was used to determine the apoptosis cells.

**Results:** Here we show that *Gdi2* is essential for embryonic development. One functional *Gdi2* allele is sufficient for murine embryo development, but complete loss of *Gdi2* leads to embryonic lethality. Developmental retardation of $Gdi2^{-/-}$ mice is apparent at E10.5 to E14.5, with no viable $Gdi2^{-/-}$ embryos detected after E14.5. Histological analysis revealed extensive cell death and cell loss in $Gdi2^{-/-}$ embryos. Apoptosis was confirmed by staining with cleaved easpase-3, suggesting that *Gdi2* maintain homeostasis by regulating the apoptosis of the cells. There was no significant difference in cytokine production and survival between wild-type and $Gdi2^{+/-}$ mice after LPS challenge.

**Discussion:** These findings suggest that one *Gdi2* allele is sufficient to maintain function. However, the detailed molecular mechanism underlying Gdi2 in regulating the embryonic development needs further identification.

*Corresponding author. Gchen14@uthsc.edu (G.-Y. Chen).

Author contributions

G.C. designed the experiments. Y.W., D.Y., and G.C. conducted the experiments. G.C. wrote the paper.

6. Materials availability

Materials are available from the corresponding author upon reasonable request, but may require a Material Transfer Agreement.

Declaration of competing interest

The authors declare no conflicts of interest or financial interests.

Appendix A. Supplementary data

Supplementary data to this article can be found online at https://doi.org/10.1016/j.placenta.2022.05.005.

**Keywords**

GDI2; RAB; Embryonic lethality; Apoptosis; Bacterial infection

## 1. Introduction

GDP dissociation inhibitor (GDI) binds to Rab GTPase in the GDP-bound inactive form to retrieve it from the cell membrane and maintain a soluble pool of inactive protein [1]. To date, more than 70 mammalian Rab proteins have been identified [2]. Some Rab proteins are expressed in specific tissues or stages of development, while others are ubiquitously expressed [2]. Each Rab protein has a characteristic subcellular distribution [3].

The GDI family includes GDI1 and GDI2 proteins. GDI1 is expressed primarily in neural and sensory tissues, whereas GDI2 is ubiquitously expressed [4]. The function of GDI1 has been extensively studied. *Gdi1*-deficient mice are fertile but show impairment in tasks requiring formation of short-term temporal associations, in addition to less aggression and altered social behavior [5]. Dysregulation of GDI2 has been reported in many different cancers, including pancreatic carcinoma [6], ovarian cancer [7,8], gastric cancer [9], thyroid carcinoma [10], hematopoiesis and leukemogenesis [11] and esophageal squamous cell carcinoma [12]. GDI2 has also been identified as a suppressor of bladder cancer metastasis [13]. Reduced expression of GDI2 is associated with decreased survival of bladder cancer patients [14]; restoration of GDI2 expression suppressed metastasis without affecting primary tumor growth in animal models or growth in culture [13,15,16]. GDI2 appears to suppress metastasis by modulating GTPase signaling [17]. Loss of GDI2 in tumor cells alters tumor cell-TAM receptor crosstalk to enhance both local inflammation and tumor cell invasion and growth [15], leading to secretion of inflammatory cytokines by macrophages that promote metastatic growth of tumor cells.

Recently, we found that GDI2 bound to the ITIM domain of Siglec-G under normal homeostasis, whereas Rab1a was recruited to the ITIM domain during bacterial infection [18]. Therefore, GDI2 and Rab1a may regulate the immune response through interaction with the ITIM domain during bacterial infection. However, the regulation of the inflammatory response by GDI2 in vivo and its regulatory mechanism remain unknown. In this study, we examined the function of *Gdi2* in vivo by generating a *Gdi2* null mutant mouse with a trapped *Gdi2* gene. Homozygous deletion of the *Gdi2* gene resulted in early embryonic lethality, and GDI2 protein was expressed during early post-implantation development, suggesting a critical role for GDI2 in the transport of materials between organelles in eukaryotic cells.

## 2. Methods

### 2.1. Reagents

Anti-Gdi2 antibody, anti-cleaved caspase-3 antibody and LPS (from *E. coli* 055:B5) were purchased from Sigma-Aldrich (Burlington, MA). β-actin (catalog no. sc-1615) antibody

was purchased from Santa Cruz Biotechnology (Dallas, TX). X-gal was obtained from Thermo Fisher Scientific (Waltham, MA).

### 2.2. Generation of Gdi2 mutant mice

Gene disruption was caused by insertion of the retroviral gene trap vector ROSAFARY. The polyA trap module of the ROSAFARY17 gene trap vector (which forms a fusion transcript with exons 3' to the insertion) is flanked by FRT sites and was removed during analysis by breeding onto ROSA26Flper mice. Genotyping was determined by PCR analysis of DNA from tail biopsies.

## 3. PCR

Aliquots of 0.1 μg (10 μl) of DNA were mixed with 10 μl of 2x GoTaq green master mix buffer (Promega, Madison, WI) and 10 pmol of each primer. PCR amplification was carried out at 96 °C for 2 min, with 35 cycles of 96 °C for 10 s, 55 °C for 30 s, and 72 °C for 60 s. To screen for homologous recombination, the following primers were used: P1: 5′-GTAGCACTGACCTTCAGCGTG -3′ and P2: 5′-GCCATGTCACAGATCATC-3'. The wild-type allele produced no band, and the mutant allele produced a 760-bp band. The following primers were also used: P1: 5′- GTAGCACTGACCTTCAGCGTG -3′ and P3: 5′- CATCTTCACCAACTGACCTTGAA -3'. The wild-type allele produced a 208-bp band; the mutant allele produced no band.

### 3.1. X-gal staining

X-gal staining of tissues was performed using standard procedures. Embryos were embedded in OCT compound and cryosectioned at 8 μm. Cryosections were fixed in X-gal fixation buffer (0.1 M phosphate buffer, pH 7.3, 5 mM EGTA, 2 mM $MgCl_2$, 0.2% glutaraldehyde) for 15 min, washed 3 times with X-gal wash buffer (0.1 M phosphate buffer, pH 7.3, 2 mM $MgCl_2$), and stained overnight at 37 °C in X-gal staining buffer (0.1 M phosphate buffer, pH 7.3, 2 mM $MgCl_2$, 5 mM $K_4Fe(CN)_6$,$3H_2O$, 5 mM $K_3Fe(CN)_6$, 1 mg/ml X-gal). Stained sections were washed 3 times with X-gal wash buffer and mounted in Aquatex (Merck, Kenilworth, NJ). Images were acquired with an EVOS FL Auto Imaging System (Thermo Fisher Scientific).

### 3.2. TUNEL staining

TUNEL staining was performed using an ApopTag Peroxidase In Situ Apoptosis Detection Kit (S7100, Chemicon, Temecula, CA) according to the manufacturer's instructions.

### 3.3. Experimental animal models

All mice used were 6–8 weeks of age. Age- and sex-matched wild-type littermates were used as controls for *Gdi2*$^{+/-}$ or *Gdi2*$^{-/-}$ mice. All animal procedures were approved by the Animal Care and Use Committee of University of Tennessee Health Science Center. Wild-type C57BL/6J mice were obtained from The Jackson Laboratory (Bar Harbor, ME). *Gdi2* mutant mice were obtained from the Mutant Mouse Regional Resource Center (MMRRC) at UC Davis.

### 3.4. Immunoblotting

Embryos lysates were prepared in lysis buffer (20 mM Tris-HCl, 150 mM NaCl, 1% Triton X-100, pH 7.6, including protease inhibitors, 1 μg $ml^{-1}$ leupeptin, 1 μg $ml^{-1}$ aprotinin and 1 mM phenylmethylsulfonyl fluoride), sonicated, centrifuged at 13,000 rpm for 5 min and then applied for Western blot analysis. The concentration of running gel was 10%. After blocking, the blots were incubated with primary antibody (1:1000 dilution). After incubation with the second antibody (HRP-conjugated goat anti-rabbit IgG) (1:5000 dilution), the signal was detected with an ECL kit (Santa Cruz, CA).

### 3.5. Histology and immunohistochemistry

Wild-type and mutant mouse embryos were fixed in 4% paraformaldehyde, dehydrated, and embedded in paraffin according to the standard procedure. The embryos were sectioned at 5-μm thickness and stained with H&E or incubated with anti-Gdi2 antibody for 1 h at room temperature. The sections were washed in PBS and subsequently incubated with horseradish peroxidase (HRP)-conjugated goat anti-rabbit antibody for 30 min at room temperature. After the sections were washed with PBS, slides were developed with 3,3′-diaminobenzidine and counterstained with hematoxylin. For the negative control, immunohistochemical staining was performed without the primary antibody. No significant staining was observed in the negative control (data not shown).

### 3.6. Measurement of inflammatory cytokines

Blood samples were obtained at indicated time points, and cytokines in the serum were determined using a mouse cytokine bead array designed for inflammatory cytokines (BD Biosciences, 552364, Franklin Lakes, NJ).

### 3.7. Statistical analysis

The differences in cytokine concentrations were analyzed by two-tailed t-tests in single pairwise comparisons calculated with Excel (Microsoft). Data are shown as the mean ± SD. n. s., not significant.

## 4. Results

### 4.1. Generation of the Gdi2 mutant mouse

To determine the function of *Gdi2* in vivo, we generated *Gdi2* mutant mice by blastocyst injection of a *Gdi2*-trapped embryonic stem cell clone (S1-11F1, Soriano). Gene disruption was caused by insertion of the retroviral gene trap vector, reverse orientation splice acceptor for array (ROSAFARY), containing a promoterless reporter gene encoding β-galactosidase. Selection for expression of the gene requires transcription from an endogenous cellular promoter. Staining for β-galactosidase activity reveals the mutation and activity of the target gene. A detailed description of the methods used for gene trap mutagenesis has been reported previously [19,20]. The gene trap vector ROSAFARY in the S1-11F1 ES cell line was inserted between exons 3 and 4 of the *Gdi2* gene; the point of insertion was confirmed by PCR and DNA sequencing (Figs. 1 and 2 and Supplementary Figs. 1 and 2). Offspring

were genotyped by PCR analyses using primers 1 and 2 for the knockout and primers 1 and 3 for the wild-type (Fig. 1).

Chimeric male offspring were then mated to wild-type C57Bl/6 mice to test for germline transmission of the disrupted *Gdi2* allele. Heterozygous *Gdi2*$^{+/-}$ mice were viable and displayed no obvious abnormality in weight or fertility during a 12-month observation period. To remove contaminating background heterozygosity, we backcrossed *Gdi2*$^{+/-}$ mice more than 10 generations with C57BL/6.

### 4.2. Gdi2 expression in mouse embryos

Since the expression of β-galactosidase is controlled by the endogenous *Gdi2* gene promoter, we used β-galactosidase expression in *Gdi2*$^{+/-}$ mice to document the expression pattern of *Gdi2* in mouse embryos. X-gal staining of cryosections of *Gdi2*$^{+/+}$ and *Gdi2*$^{+/-}$ E7 embryos showed that *Gdi2* is ubiquitously expressed in whole embryos (Fig. 3), as previously reported [4]. Wild-type embryo sections were used as controls.

To investigate endogenous GDI2 protein expression, we collected, sectioned, and immunostained wild-type E7 embryos with anti-GDI2 antibodies. GDI2 was ubiquitously expressed in the whole embryo (Fig. 3). Corresponding sections were stained with secondary antibody as negative controls. E7 mouse embryo sections were also stained with hematoxylin and eosin (H&E) (Fig. 3).

The pattern of β-galactosidase staining in *Gdi2*$^{+/+}$ mouse embryos was similar to the pattern of GDI2 antibody staining observed in wild-type embryos. Both staining methods indicated that *Gdi2* is ubiquitously expressed in whole embryos. These results show that GDI2 protein expression was consistent with the detected *Gdi2* β-galactosidase activity shown in Fig. 3.

### 4.3. Gdi2 deficiency leads to embryonic lethality

To generate *Gdi2*$^{-/-}$ mice, we intercrossed heterozygous *Gdi2*$^{+/-}$ mice. The offspring's genotypes were identified two weeks after birth. None of the 429 offspring was homozygous mutants (*Gdi2*$^{-/-}$) (total: 429; *Gdi2*$^{+/+}$: 172; *Gdi2*$^{+/-}$: 257), and no increased neonatal mortality was observed in the initial 2 weeks after birth. The ratio of wild-type to heterozygous mice was 0.67, in accordance with Mendel's law. These results indicate *Gdi2* is essential for embryonic development. One functional *Gdi2* allele is sufficient for murine embryonic development, but complete loss of *Gdi2* leads to embryonic lethality.

To characterize the effect of *Gdi2* mutation on embryonic development, we performed timed matings between *Gdi2* heterozygous mice. Embryos at embryonic day (E) 10.5, 14.5, 15.5 and 16.5 were collected from *Gdi2*$^{+/-}$ breeding mice and genotyped by PCR analysis using genomic DNA (Fig. 4). At E10.5, *Gdi2*$^{+/+}$, *Gdi2*$^{+/-}$, and *Gdi2*$^{-/-}$ embryos were recovered and viable. However, developmental retardation of Gdi2$^{-/-}$ embryos became apparent at E14.5, E15.5 and E16.5. No viable *Gdi2*$^{-/-}$ embryos were recovered after E14.5, suggesting that embryonic lethality occurs between E10.5 to E14.5.

### 4.4. GDI2 protein deficiency in knockout mice

Wild-type and mutant alleles were assessed by PCR of DNA isolated from mice, and the disruption of GDI2 expression was confirmed by Western blot analysis, with β-actin used as a loading control (Fig. 5). E10.5 embryos were collected and genotyped by PCR. *Gdi2*$^{+/+}$ and *Gdi2*$^{-/-}$ embryos were lysed and used for Western blot analysis with anti-Gdi2 antibody. GDI2 protein was absent in *Gdi2*$^{-/-}$ embryos, indicating functional loss of *Gdi2*.

### 4.5. Increased apoptosis in the liver of Gdi2 mutant mice

Histological analysis revealed extensive cell death and cell loss in *Gdi2*$^{-/-}$ embryos (Fig. 6). To determine the cause of embryonic lethality in mutant embryos, we examined cell death in E12.5 liver. Terminal deoxynucleotidyl transfer-mediated dUTP-biotin end labeling (TUNEL) staining was used to detect apoptotic cells in wild-type and *Gdi2*$^{-/-}$ liver sections. Compared to wild-type, *Gdi2*$^{-/-}$ liver sections contained numerous TUNEL-positive cells, indicating significant apoptosis in *Gdi2*$^{-/-}$ liver.

Caspase-3, a cysteine protease, controls both cytoplasmic and nuclear events associated with Fas-mediated apoptosis by cleaving a variety of key cellular proteins; cleaved Caspase-3 is a marker for activated caspase-3 and apoptosis [21]. To confirm apoptosis occurred in *Gdi2*$^{-/-}$ embryos, we performed cleaved caspase-3 staining in wild-type and *Gdi2*$^{-/-}$ embryo liver sections (Fig. 7). Compared to wild-type, *Gdi2*$^{-/-}$ liver sections contained extensive cleaved caspase-3-positive cells, confirming the significant apoptosis in *Gdi*$^{-/-}$ liver identified by TUNEL staining.

### 4.6. One Gdi2 allele is sufficient for resistance to LPS challenge

To investigate whether GDI2 plays a role during bacterial infection, we challenged wild-type and *Gdi2*$^{+/-}$ mice with 10 mg/kg lipopolysaccharide (LPS) and then collected serum from the mice. As shown in Fig. 8, both *Gdi2*$^{+/-}$ and wild-type mice produced similar levels of cytokines following LPS stimulation. There was no significant difference in survival after LPS challenge (data not shown).

## 5. Discussion

The transfer of material between organelles in eukaryotic cells is predominantly mediated by vesicular transport. GTP binding proteins regulate vesicular traffic at many stages of the exocytic and endocytic transport pathways. Rab GTPases are small GTP-binding proteins in the Ras superfamily. After a vesicle fusion event, Rab is returned to its membrane of origin by GDI. GDI proteins regulate the GDP-GTP exchange reaction of Rab family members that are involved in vesicular trafficking of molecules between cellular organelles. GDIs slow the rate of dissociation of GDP from Rab proteins and release GDP from membrane-bound Rab [2,22].

To date, two forms of GDI, namely GDI1 and GDI2, have been identified. GDI2 comprises 1340 nucleotides and encodes a protein GDI2 with a molecular weight of 49KD [4]. We have previously shown that GDI2 may regulate the immune response through interaction with the ITIM domain during bacterial infection in vitro [18]. To further investigate the

function of GDI2 in vivo, we generated mice with a trapped *Gdi2* gene and uncovered a novel role for *Gdi2* during early embryonic development. None of 429 genotyped pups from *Gdi2* heterozygous mating pairs showed homozygous deletion of the *Gdi2* allele. We also did not detect any viable *Gdi2* null embryos between developmental days 14.5–16.5, indicating a severe early embryonic defect caused by the complete loss of *Gdi2* function. However, one functional *Gdi2* allele is sufficient for murine embryo development, indicated by the expected frequency of heterozygous offspring.

The lack of differences in cytokine production and survival between wild-type and $Gdi2^{+/-}$ mice after LPS challenge suggest that one *Gdi2* allele is sufficient to maintain function. To further explore the function of *Gdi2* in bacterial infection and embryonic development, we will need to use a conditional knockout strategy [23].

Apoptosis is a fundamental process for normal development of multicellular organism, and is important in the regulation of the immune system, normal morphogenesis and maintenance of homeostasis. For example, non-functional or autoreactive lymphocytes are eliminated through apoptosis. Fas, a member of the tumor necrosis factor receptor (TNFR) family, can trigger cell death and is essential for lymphocyte homeostasis. GDI2 is a target for caspase cleavage upon apoptotic induction by Fas [24,25]. GDI2 knockdown inhibitors the cell cycle and promotes apoptosis in prostate cells [26]. In this study, we found that extensive cell loss and apoptosis in $Gdi2^{-/-}$ embryos with TUNEL and cleaved caspase-3 staining. These results suggested that *Gdi2* maintain homeostasis by regulating the apoptosis of the cells and might via the p75NTR signaling pathway which was recently reported [26]. Further studies are required to show how GDI2 mediates the pathway of death and growth and the molecular relationship between them.

## Supplementary Material

Refer to Web version on PubMed Central for supplementary material.

## Acknowledgments

We thank Dr. Courtney Bricker-Anthony for editing the text of a draft of this manuscript.

### Funding and additional information

This work was supported by Grant R01AI137255 from the National Institutes of Health.

## References

[1]. Takai Y, Sasaki T, Matozaki T, Small GTP-binding proteins, Physiol. Rev 81 (1) (2001) 153–208. [PubMed: 11152757]

[2]. Pfeffer SR, Rab GTPases: specifying and deciphering organelle identity and function, Trends Cell Biol. 11 (12) (2001) 487–491. [PubMed: 11719054]

[3]. Zerial M, McBride H, Rab proteins as membrane organizers, Nat. Rev. Mol. Cell Biol 2 (2) (2001) 107–117. [PubMed: 11252952]

[4]. Fagerberg L, Hallstrom BM, Oksvold P, Kampf C, Djureinovic D, Odeberg J, Habuka M, Tahmasebpoor S, Danielsson A, Edlund K, Asplund A, Sjostedt E, Lundberg E, Szigyarto CA, Skogs M, Takanen JO, Berling H, Tegel H, Mulder J, Nilsson P, Schwenk JM, Lindskog C, Danielsson F, Mardinoglu A, Sivertsson A, von Feilitzen K, Forsberg M, Zwahlen M, Olsson

I, Navani S, Huss M, Nielsen J, Ponten F, Uhlen M, Analysis of the human tissue-specific expression by genome-wide integration of transcriptomics and antibody-based proteomics, Mol. Cell. Proteomics : MCP 13 (2) (2014) 397–406. [PubMed: 24309898]

[5]. D'Adamo P, Welzl H, Papadimitriou S, Raffaele di Barletta M, Tiveron C, Tatangelo L, Pozzi L, Chapman PF, Knevett SG, Ramsay MF, Valtorta F, Leoni C, Menegon A, Wolfer DP, Lipp HP, Toniolo D, Deletion of the mental retardation gene Gdil impairs associative memory and alters social behavior in mice, Hum. Mol. Genet 11 (21) (2002) 2567–2580. [PubMed: 12354782]

[6]. Sun ZL, Zhu Y, Wang FQ, Chen R, Peng T, Fan ZN, Xu ZK, Miao Y, Serum proteomic-based analysis of pancreatic carcinoma for the identification of potential cancer biomarkers, Biochim. Biophys. Acta 1774 (6) (2007) 764–771. [PubMed: 17507299]

[7]. Zhang XY, Hong SS, Zhang M, Cai QQ, Zhang MX, Xu CJ, Proteomic alterations of fibroblasts induced by ovarian cancer cells reveal potential cancer targets, Neoplasma 65 (1) (2018) 104–112. [PubMed: 28857608]

[8]. Lee DH, Chung K, Song JA, Kim TH, Kang H, Huh JH, Jung SG, Ko JJ, An HJ, Proteomic identification of paclitaxel-resistance associated hnRNP A2 and GDI 2 proteins in human ovarian cancer cells, J. Proteome Res 9 (11) (2010) 5668–5676. [PubMed: 20858016]

[9]. Bai Z, Ye Y, Liang B, Xu F, Zhang H, Zhang Y, Peng J, Shen D, Cui Z, Zhang Z, Wang S, Proteomics-based identification of a group of apoptosis-related proteins and biomarkers in gastric cancer, Int. J. Oncol 38 (2) (2011) 375–383. [PubMed: 21165559]

[10]. Zou J, Qian J, Fu H, Yin F, Zhao W, Xu L, MicroRNA15b5p exerts its tumor repressive role via targeting GDI2: a novel insight into the pathogenesis of thyroid carcinoma, Mol. Med. Rep 22 (4) (2020) 2723–2732. [PubMed: 32945458]

[11]. Gu H, Chen C, Hao X, Wang C, Zhang X, Li Z, Shao H, Zeng H, Yu Z, Xie L, Xia F, Zhang F, Liu X, Zhang Y, Jiang H, Zhu J, Wan J, Wang C, Weng W, Xie J, Tao M, Zhang CC, Liu J, Chen GQ, Zheng J, Sorting protein VPS33B regulates exosomal autocrine signaling to mediate hematopoiesis and leukemogenesis, J. Clin. Invest 126 (12) (2016).

[12]. Kashyap MK, Harsha HC, Renuse S, Pawar H, Sahasrabuddhe NA, Kim MS, Marimuthu A, Keerthikumar S, Muthusamy B, Kandasamy K, Subbannayya Y, Prasad TS, Mahmood R, Chaerkady R, Meltzer SJ, Kumar RV, Rustgi AK, Pandey A, SILAC-based quantitative proteomic approach to identify potential biomarkers from the esophageal squamous cell carcinoma secretome, Cancer Biol. Ther 10 (8) (2010) 796–810. [PubMed: 20686364]

[13]. Gildea JJ, Seraj MJ, Oxford G, Harding MA, Hampton GM, Moskaluk CA, Frierson HF, Conaway MR, Theodorescu D, RhoGDI2 is an invasion and metastasis suppressor gene in human cancer, Cancer Res. 62 (22) (2002) 6418–6423. [PubMed: 12438227]

[14]. Theodorescu D, Sapinoso LM, Conaway MR, Oxford G, Hampton GM, Frierson HF Jr., Reduced expression of metastasis suppressor RhoGDI2 is associated with decreased survival for patients with bladder cancer, Clin. Cancer Res 10 (11) (2004) 3800–3806. [PubMed: 15173088]

[15]. Said N, Sanchez-Carbayo M, Smith SC, Theodorescu D, RhoGDI2 suppresses lung metastasis in mice by reducing tumor versican expression and macrophage infiltration, J. Clin. Invest 122 (4) (2012) 1503–1518. [PubMed: 22406535]

[16]. Ahmed M, Sottnik JL, Dancik GM, Sahu D, Hansel DE, Theodorescu D, Schwartz MA, An osteopontin/CD44 Axis in RhoGDI2-mediated metastasis suppression, Cancer Cell 30 (3) (2016) 432–443. [PubMed: 27593345]

[17]. Griner EM, Dancik GM, Costello JC, Owens C, Guin S, Edwards MG, Brautigan DL, Theodorescu D, RhoC is an unexpected target of RhoGDI2 in prevention of lung colonization of bladder cancer, Mol. Cancer Res. : MCR 13 (3) (2015) 483–492. [PubMed: 25516960]

[18]. Wu Y, Yang D, Chen GY, The role of the Siglec-G ITIM domain during bacterial infection, Cell. Mol. Biol 67 (4) (2021) 163–169. [PubMed: 34933715]

[19]. Chen WV, Soriano P, Gene trap mutagenesis in embryonic stem cells, Methods Enzymol. 365 (2003) 367–386. [PubMed: 14696359]

[20]. Friedrich G, Soriano P, Insertional mutagenesis by retroviruses and promoter traps in embryonic stem cells, Methods Enzymol. 225 (1993) 681–701. [PubMed: 8231879]

[21]. Zheng TS, Schlosser SF, Dao T, Hingorani R, Crispe IN, Boyer JL, Flavell RA, Caspase-3 controls both cytoplasmic and nuclear events associated with Fas-mediated apoptosis in vivo, Proc. Natl. Acad. Sci. U. S. A 95 (23) (1998) 13618–13623. [PubMed: 9811849]

[22]. Seabra MC, Wasmeier C, Controlling the location and activation of Rab GTPases, Curr. Opin. Cell Biol 16 (4) (2004) 451–457. [PubMed: 15261679]

[23]. Le Y, Sauer B, Conditional gene knockout using ere recombinase, Methods Mol. Biol 136 (2000) 477–485. [PubMed: 10840735]

[24]. Na S, Chuang TH, Cunningham A, Turi TG, Hanke JH, Bokoch GM, Danley DE, D4-GDI, a substrate of CPP32, is proteolyzed during Fas-induced apoptosis, J. Biol. Chem 271 (19) (1996) 11209–11213. [PubMed: 8626669]

[25]. Essmann F, Wieder T, Otto A, Muller EC, Dorken B, Daniel PT, GDP dissociation inhibitor D4-GDI (Rho-GDI2), but not the homologous rho-GDI 1, is cleaved by caspase-3 during drug-induced apoptosis, Biochem. J 346 Pt 3 (2000) 777–783. [PubMed: 10698706]

[26]. Liu C, Wang W, Lin P, Xie H, Jiang S, Jia H, Li R, Wang N, Yu X, GDI2 is a target of paclitaxel that affects tumorigenesis of prostate cancer via the p75NTR signaling pathway, Biochem. Biophys. Res. Commun 562 (2021) 119–126. [PubMed: 34051575]

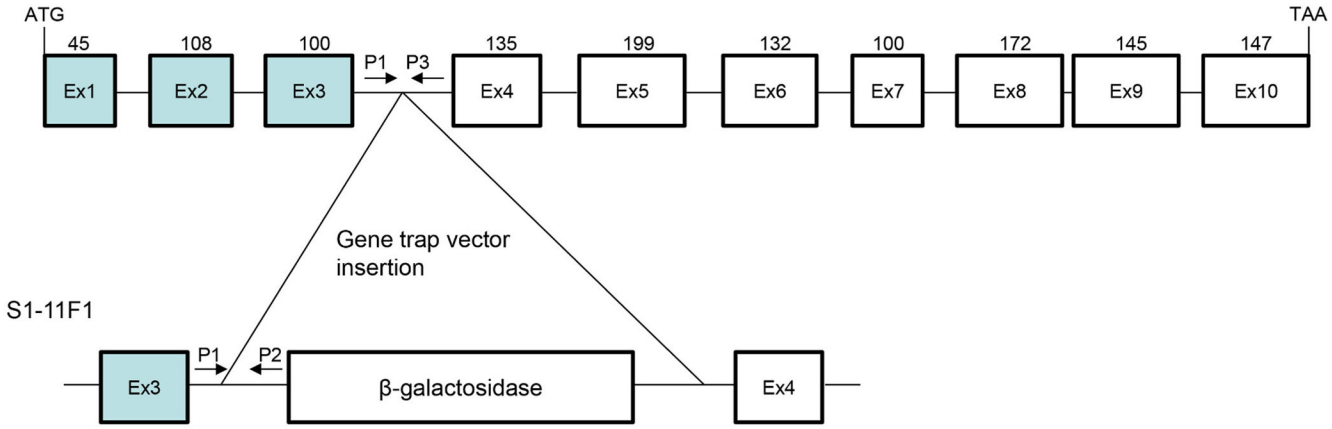


**Fig. 1. Localization of the gene trap vector interrupting the *Gdi2* gene.**

Genomic exon organization of *Gdi2* gene. Exons (Ex). Numbers above exons correspond to *Gdi2* cDNA. The second row shows a diagram of the mutated allele of the *Gdi2* gene; a β-galactosidase gene was inserted between exons 3 and 4 of the *Gdi2* gene. The three primers (P1, P2, and P3) used for genotyping are shown.

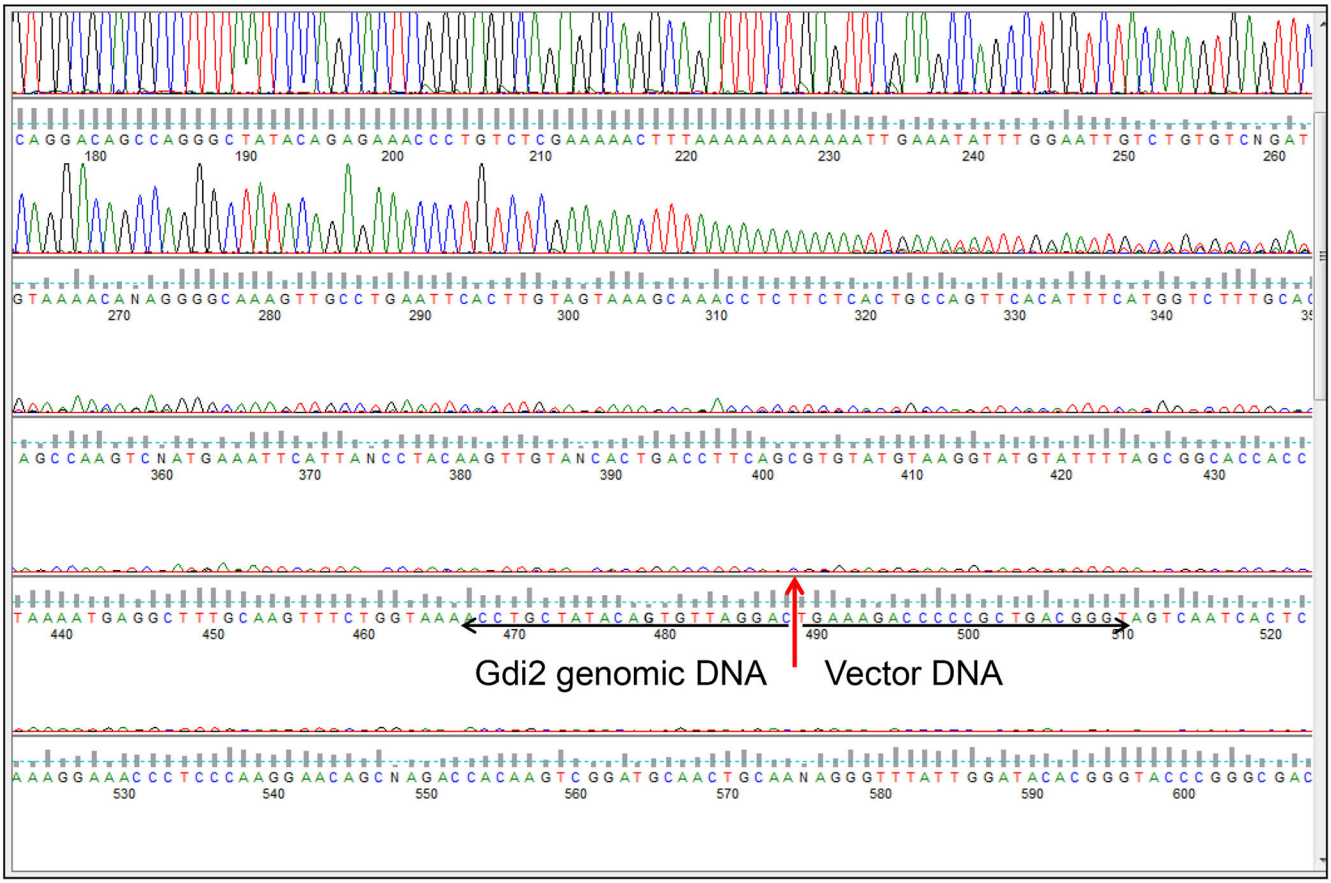


**Fig. 2. DNA sequence of *Gdi2* insertion site.**

The nucleotide sequence near the splice junction joining the *Gdi2* exon 3 splice donor to the splice acceptor of the vector is indicated. The red arrow indicates the insertion site between the *Gdi2* genomic DNA sequence and vector DNA sequence.

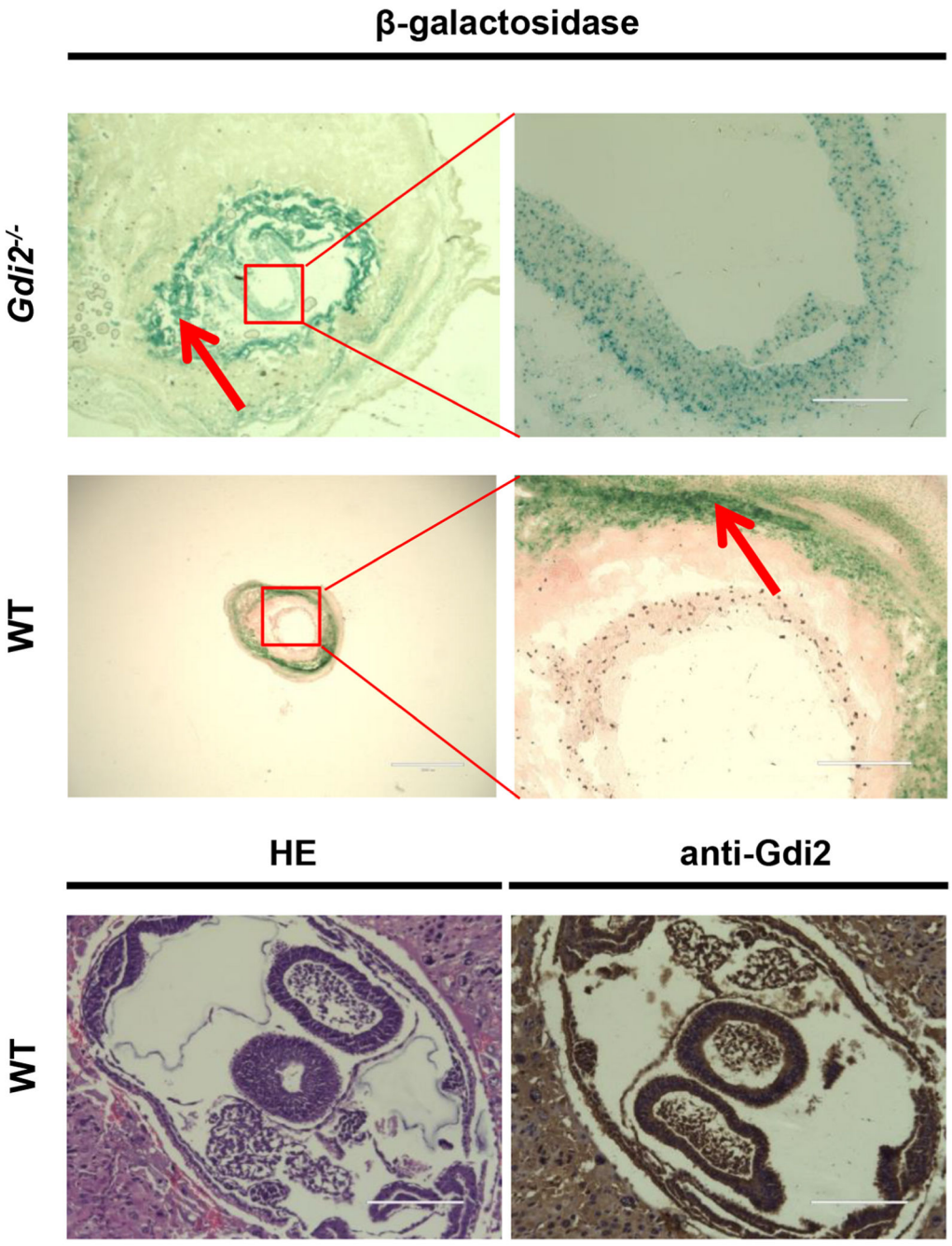


**Fig. 3. Expression of *Gdi2* in embryos.**

X-gal staining of cryosections of *Gdi2*$^{-/-}$ and wild-type (WT) embryos. Corresponding WT sections serve as negative controls for specific X-gal staining in knockout mice. Higher magnification images are also shown. Experiments in this figure were performed in duplicate, and representative images are shown. Hematoxylin and eosin (HE) staining of WT embryo cryosections was performed. WT embryo cryosections were also stained with anti-Gdi2 antibody and counterstained with hematoxylin. Bar: 200 μM. The red arrow indicates non-specific staining.

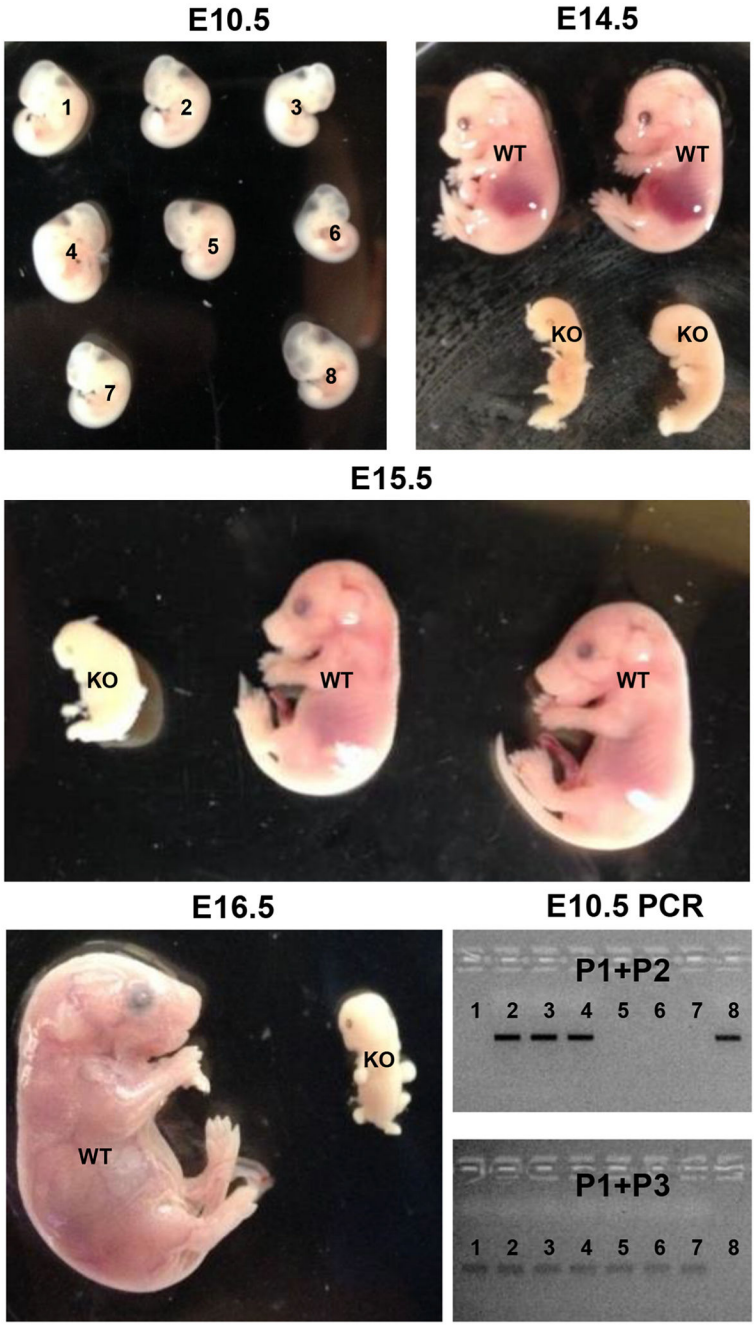


**Fig. 4. *Gdi2* mutant resulted in embryonic lethality.**

Representative images of E10.5, E14.5, E15.5 and E16.5 embryos of the indicated genotypes. PCR genotyping results for the E10.5 embryos are shown using the indicated allele-specific primers. WT, wild-type; KO, Knockout.

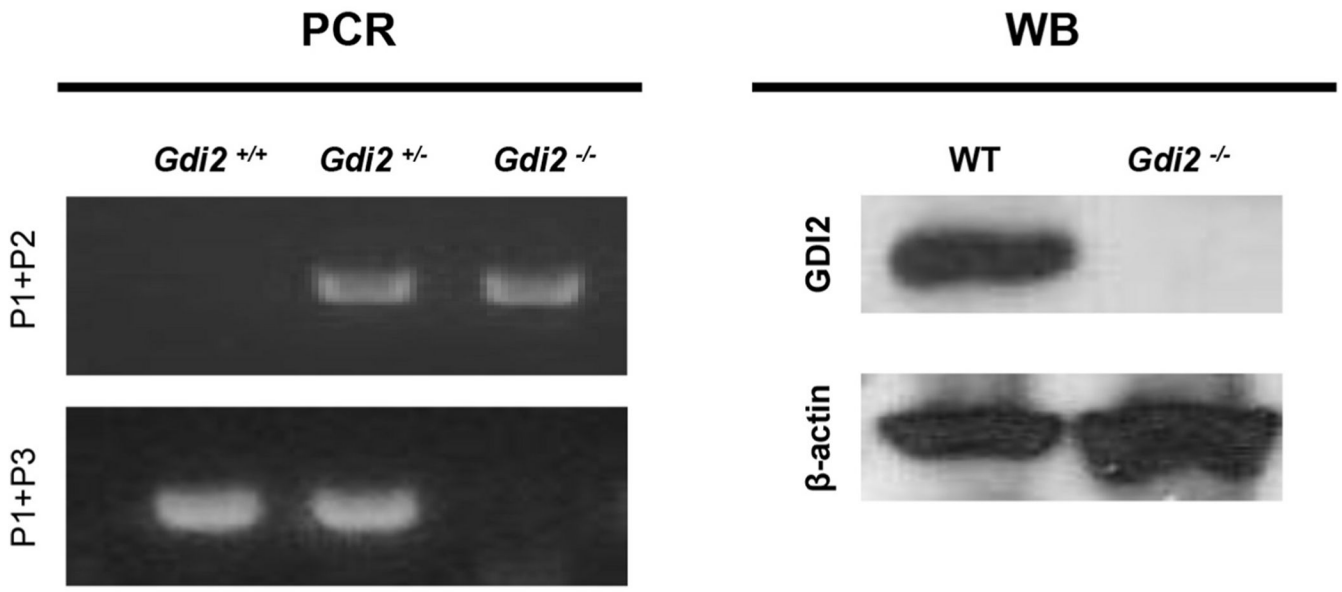


**Fig. 5. PCR and Western blot analyses of Gdi2.**

Representative PCRs show mouse genotypes. Loss of *Gdi2* in S1-11F1-derived mice is shown. Proteins were extracted from embryonic tissues, separated by SDS/PAGE, and subjected to western blotting. Western blot demonstrates lack of GDI2 protein in embryo lysates of *Gdi2*$^{-/-}$ mice compared to wild-type (WT) control mice. β-actin was used as a loading control. Representative data from two independent experiments are shown.

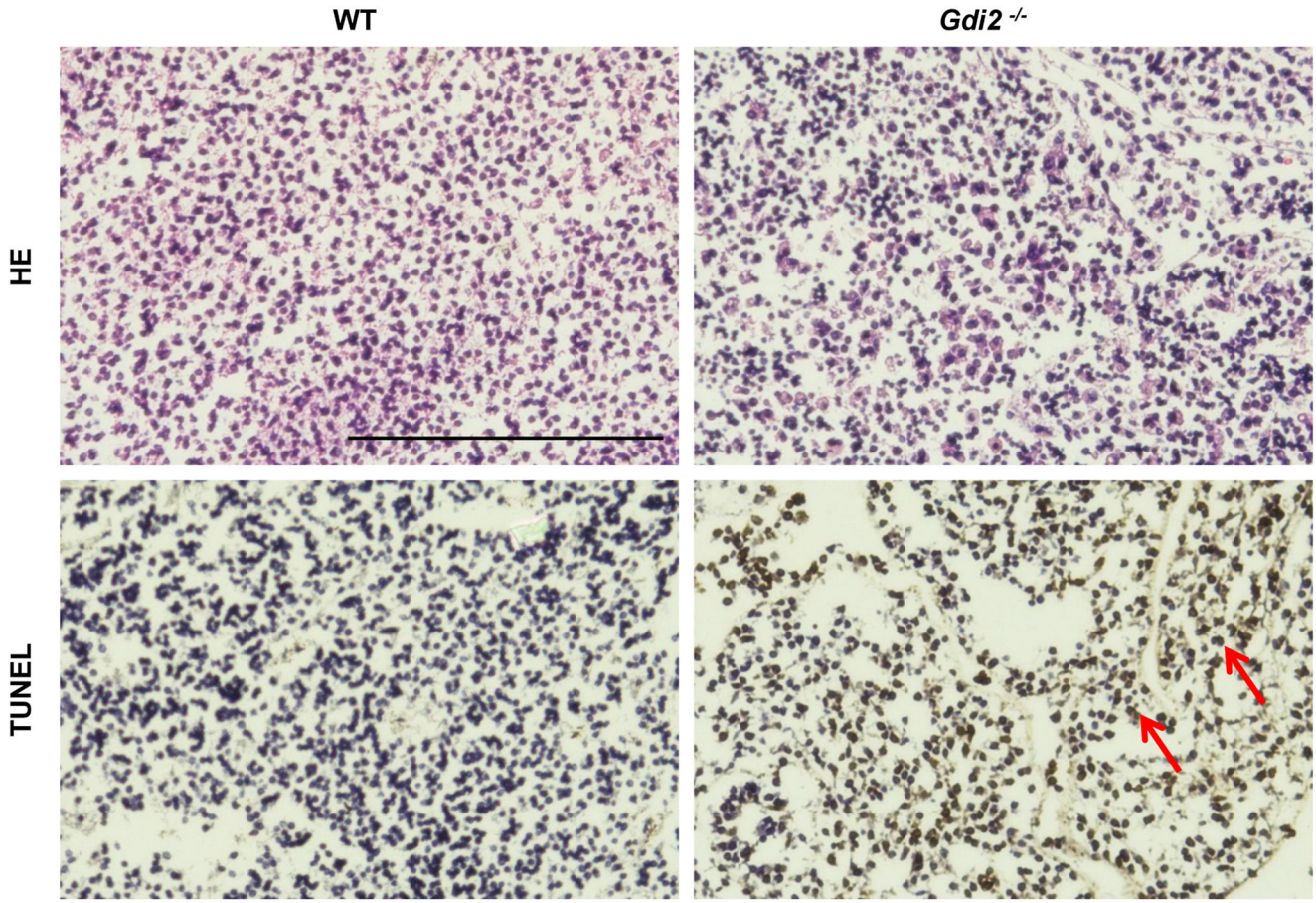


**Fig. 6. Liver histology and TUNEL staining.**

Representative cryosections from wild-type (WT) and *Gdi2*$^{-/-}$ embryo liver stained with H&E (HE) are shown. TUNEL staining was performed on WT and *Gdi2*$^{-/-}$ embryo liver cryosections; representative images are shown. Experiments in this figure were performed in duplicate. Bar: 200 μM. The red arrow indicates positive staining.

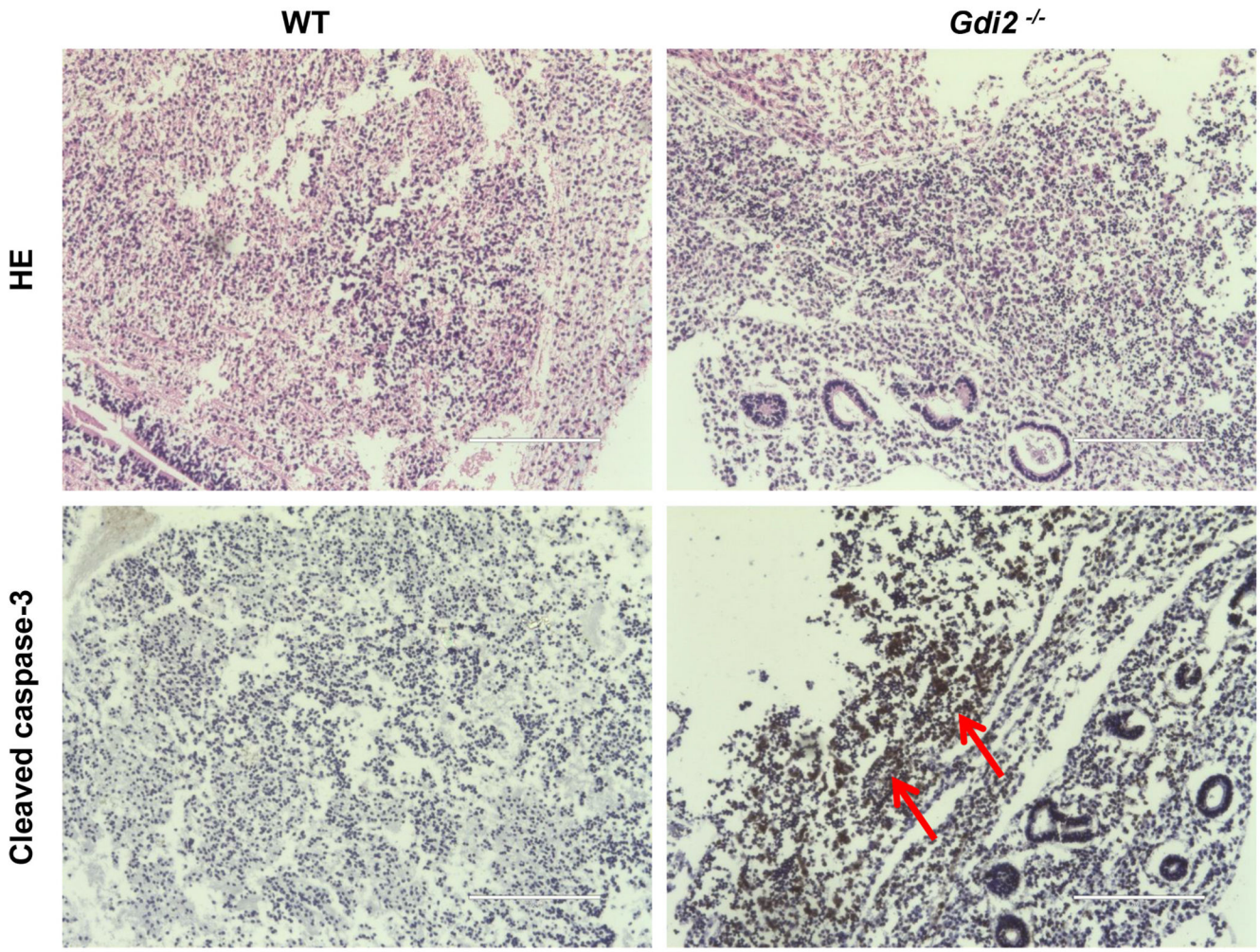


**Fig. 7. Expression of cleaved caspase-3 in embryonic tissues.**

Cryosections from wild-type (WT) and *Gdi2*$^{-/-}$ embryo liver were stained with H&E (HE). Cryosections from WT and *Gdi2*$^{-/-}$ embryo liver were stained with anti-cleaved caspase-3 antibody and counterstained with hematoxylin. Representative images are shown. Experiments in this figure were performed in duplicate. Bar: 200 μM. The red arrow indicates positive staining.

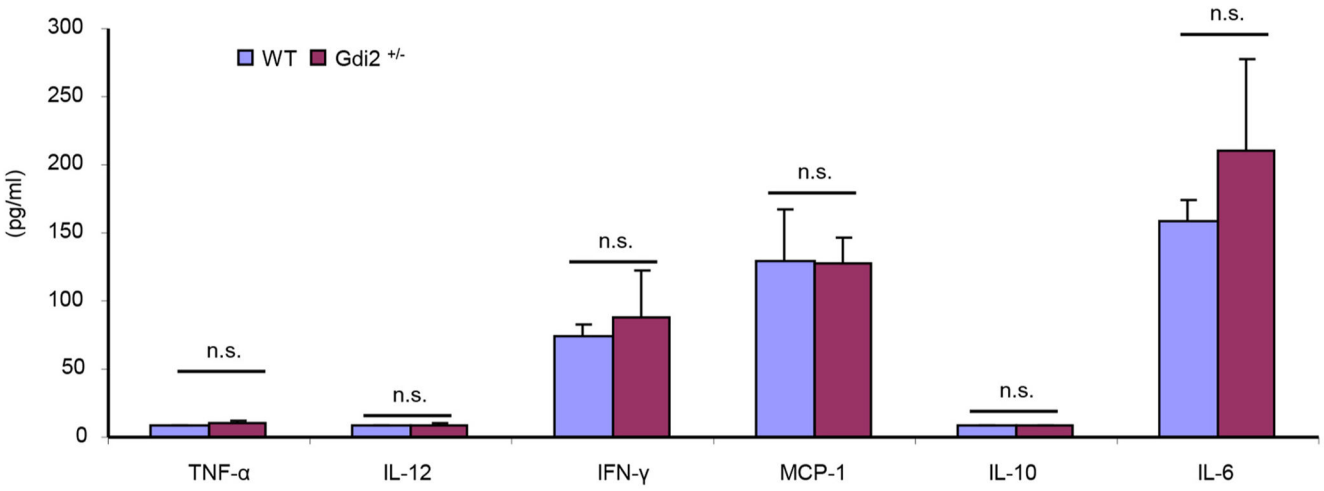


**Fig. 8. One *Gdi2* allele is sufficient for resistance to LPS challenge.**

Serum concentrations of TNF-α, IL-6, IL-12, IL-10, MCP-1 and IFN-γ at 16 h after LPS treatment (mean ± SD, n = 8). Experiments in this figure were performed in duplicate, n. s., not significant.